Damage identification of prepreg composites subject to accelerated fatigue tests

L. Pyl[1], H. Sol[1], F. Zastavnik[1], J. Gu[1], W. Van Paepegem[2], M. Kersemans[2]

[1] Department Mechanics of Materials and Constructions (MeMC), Vrije Universiteit Brussel (VUB), Pleinlaan 2, 1050 Brussels, Belgium

[2] Department of Materials Science and Engineering, Universiteit Gent (UGent), Technologiepark-Zwijnaarde 903, 9052 Zwijnaarde, Belgium

ABSTRACT

The fatigue behavior of composite materials under time-dependent loading is investigated. Fatigue is induced in test beams using an electro-magnetic shaker. The test beams made of prepreg composite materials with a layup $[(\pm45)_2]_S$ before and after fatigue loading are used as a case study for the proposed method. The averaged stiffness properties of the test specimen are monitored during the fatigue cycles by measuring the first natural frequency. The first bending mode shapes of the test beams are measured using a laser scanning vibrometer at selected fatigue stages. Based on this modal information, the (reduced) bending stiffness distribution of the test beam is identified using an inverse method.

1. INTRODUCTION

The durability of composite materials is largely influenced by the fatigue behavior under time-dependent loading. The increasing trend to use composites in primary components of among others cars, in aerospace applications and in wind turbines incites the need for fatigue assessment under dynamic loading. The appearance of matrix cracks leads to a reduction in structural stiffness. This damage will change the natural vibration characteristics. Damage identification using vibration analysis is considered in the present work. It is a faster and cheaper alternative for the test set-ups and capable of generating both uni- and multi-axial stress states.

1.1. Accelerated fatigue tests

Most of the applications of fibre-reinforced plastics were limited to the so-called secondary components of cars and in aerospace applications so far. The problem of fatigue of fibre-reinforced plastics was partially avoided and the maximum strain in composite components was arbitrarily limited to 4000 microstrain (fatigue limit for BVID: Bearly Visible Impact Damage). This threshold was so low that fatigue damage was rarely a problem and design could be limited to static loading conditions [1–3]. Increasing oil prices fortified the trend to use composite materials in the so-called primary components. Limiting the design to static loading conditions is no longer possible for these primary components with substantial weight savings. As a consequence the fatigue behavior of composites becomes an issue. Moreover a number of unforeseen failures with large composite wind turbine blades have proved that fatigue can be a problem if not properly accounted for [4], [5]. In this research project, accelerated fatigue tests on fibre-reinforced composite beams by means of electro-magnetic shakers are used for characterization of the fatigue behavior of plastics. The method, developed for beam-like structures, will further be extended for damage identification in plate-like structures. The method avoids the distinct disadvantages related to the use of the experimental tests such as (i) the limited practical use of the S-N curves based on uniaxial fatigue tests on rectangular specimens because almost all composite structures are subject to a multiaxial stress state under in-service fatigue loading [6], (ii) expensive test set-up, complex specimen geometry and the occurrence of stress concentrations at the grips in laboratory tests that generate a multiaxial stress state such as biaxial loading of a plane cruciform [7] and a combination of tension/compression and torsion on tubular specimens [8], (iii) very expensive construction of the test facilities and running of the full-scale fatigue tests.

The faster and simpler fatigue tests proposed in this article provide a lot more information in a much shorter time. Using an electro-magnetic shaker, resonance of the test specimen is induced with mode shapes causing a non-homogeneous stress state.

1.2. Local damage identification

The corresponding reduction in stiffness due to these accelerated fatigue tests is identified by measuring the amplitudes of the vibration modes of the test specimen and applying an inverse identification algorithm [9]. Test beams made of prepreg composite materials before and after fatigue loading are used as a case study for the proposed method. The stiffness properties of the test specimen are identified using a Resonalyser test [10]. A distributed stiffness scanning of the test beams is then applied. The mode shapes are measured using a laser scanning vibrometer or shearography. Based on the modal information of the first bending mode, the (reduced) bending stiffness of the test beam is identified in the inverse method.

2. ACCELERATED FATIGUE TESTING WITH ELECTRO-MAGNETIC SHAKER

With the advent of the electro-magnetic shaker, many loading cycles can be imposed in a controlled way in a short time span to have an accelerated fatigue test. A harmonic sinusoidal signal, generated by a signal generator unit, is amplified and sent to an electro-magnetic shaker (Figure 1). The test beam is clamped between rubber strips in the middle with a clamping device that is mounted on the head of the electro-magnetic shaker.

Figure 1 – Accelerated fatigue testing with an electro-magnetic shaker

The frequency of the harmonic signal can be adjusted in such a way that the beam specimen vibrates always at resonance and the mode shape has constant amplitude. The induced stresses in the beam are maximal at the clamping position and zero at the free ends of the beam.

Due to the continuous vibration excitation, the beam stiffness *EI* of the beam reduces by fatigue and hence the resonance frequency decreases progressively. The amplitude of the mode shape is monitored and the frequency of the signal generator is tuned (reduced) in such a way that the test beam is kept in resonance. The vibration amplitude is kept at a desired constant value.

By interrupting the fatigue test at well-chosen moments in time and measuring separately the amplitude distribution of the three lowest vibration modes, it is possible to calculate the evolution of the beam stiffness from point to point in function of the number of applied loading cycles.

The induced damage will lead to stiffness reduction and hence the resonance frequency will drop in value. Therefore also the mode shape will change because the most heavily loaded areas will suffer from the largest stiffness degradation. By continuously monitoring and adjusting the excitation frequency of the shaker so that the specimen keeps vibrating in resonance, the specimen will be fatigued very fast (many cycles in short time period).

3. DISTRIBUTED STIFFNESS EVALUATION

The damage is identified assuming thin beam Euler-Bernoulli (EB) behavior using both resonance frequency and mode shape information. The mode shapes need not to be mass normalised. The modal identification can be carried out based on the responses only. The case where the modal parameters are identified without knowing the loads exciting the system is called modal identification of output-only systems. The method is a linear, model based, inverse method and aims the determination of the location and quantification of the beam stiffness. The use of the information contents of the first bending mode shape is adequate enough for the identification of a complete stiffness pattern.

The time independent normal differential equation of the equilibrium in an arbitrary point in the domain of a beam vibrating in resonance at a circular frequency ω neglecting damping is:

$$\frac{d^2}{dx^2}(EI(x)\frac{d^2W(x)}{dx^2}) - \rho A(x)\omega^2 W(x) = 0 \tag{1}$$

where $W(x)$ is the arbitrary scaled modal deformation term of the associated mode shape, ρ is the specific mass and A is the area of the beam's cross section. The product ρA is the mass per unit length of the beam and can be an arbitrary function of the independent variable x. Eq. (1) can be seen as the differential equation of an EB-beam (see text books about strength of materials and constructions, Seed [11]) loaded statically with a distributed pressure $p(x) = \rho A\omega^2 W(x)$. The product EI (with E being the Young's modulus and I the moment of inertia of the beam's cross section) is called the flexural beam rigidity or 'stiffness' and its value can be an arbitrary function of the independent variable x. So the stiffness can be identified locally in an arbitrary small sub domain and is therefore called 'sub domain identification'. The - a priori unknown - distributed beam stiffness values EI are the parameters in a finite element model of the beam. The modal amplitudes of the first bending mode shape of the freely suspended composite test beam are the measured output values. The beam stiffness value in a small sub domain of the test beam is iteratively tuned in such a way that the computed modal amplitudes in the sub domain match the measured modal amplitudes. This principle comparing measured output values from an experiment on a test specimen with the computed output values of a numerical model of the same specimen loaded with the same boundary and initial values is the basic idea of an inverse method [9], [12]. The boundary conditions of a virtually isolated sub domain must be such that they represent the action of the remaining parts of the considered domain on the boundaries of the selected sub domain. The sub domain can be hence isolated without changing the stress state conditions in arbitrary points of the sub domain. The beam stiffness will be identified or 'scanned' in an arbitrary number of beam sub domains which are sufficiently small to assume constant flexural rigidity EI and constant mass per unit length ρA. The beam sub domain is in each of the two boundary points x_k and x_l subjected to prescribed transversal displacements ($\overline{W_k}$ and $\overline{W_l}$) as Dirichlet boundary conditions and prescribed bending moments ($\overline{M_k}$ and $\overline{M_l}$) as Von Neumann boundary conditions.

Eq. (1) can be transformed into an equivalent integral formulation having the same solution for the dependent variable $W(x)$. By using the weighted residual method with a virtual displacement field $\delta V(x)$ as weighting function for the differential equation, and V_k and V_l as arbitrary weighting scalars for the Von Neumann boundary conditions, the integral formulation over the sub domain $[x_k, x_l]$ is:

$$EI\int_{x_k}^{x_l}\frac{d^2W}{dx^2}\frac{d^2\delta V}{dx^2}dx = \rho A\omega^2\int_{x_k}^{x_l}W\delta V dx + \bar{M}_k\frac{d\delta V}{dx}(x_k) - \bar{M}_l\frac{d\delta V}{dx}(x_l) \tag{2}$$

The transversal displacement amplitude $W(x)$ of the modal deformation of the first mode shape is expressed in a finite element approximation as a linear combination of Lagrange shape functions $N_i(x)$ multiplied with W_i, the value of $W(x)$ in the node i. The latter is one of the M nodal points of a regular grid in which the beam sub domain $[x_k, x_l]$ is divided into.

Only the transversal displacement amplitude $W(x)$ is taken as a degree of freedom in the finite element formulation. This is possible because, unlike in traditional beam finite element formulations, slope continuity is not required because the beam sub domains are not assembled and thus the derivative of $W(x)$ is redundant.

Using the same interpolation functions N_i to express the virtual field δV and replacing the Cartesian coordinate x by a local homogenized coordinate ξ having values from -1 towards +1 in the considered sub domain, an expression can be obtained which allows to evaluate the stiffness EI as a function of W_i, boundary conditions and known beam parameters:

$$EI = \frac{\rho A \omega^2 L^{e4} B_{ij} W_i W_j + 4 L^{e2} \bar{M}_1 W_i \frac{dN_i}{d\xi}(-1) - 4 L^{e2} \bar{M}_M W_i \frac{dN_i}{d\xi}(1)}{16 A_{ij} W_i W_j} \tag{5}$$

with:

$$A_{ij} = \int_{-1}^{1} \frac{d^2 N_i}{d\xi^2} \frac{d^2 N_j}{d\xi^2} . d\xi$$

$$B_{ij} = \int_{-1}^{1} N_i N_j \, d\xi$$

$$i = 2, 3, ... M - 1$$

$$j = 1, 2, ... M$$

$$L_e : \text{length of the considered beam sub domain}$$

The transversal displacement amplitude W_i is assumed to be measured in all the interior points ($i = 2$, M-1) of the selected beam sub domain. Thus the evaluation of Eq. (5) requires in addition the values ($\overline{M_1}$ and $\overline{M_M}$) and (W_1 and W_M) at the boundaries of the sub domain. The reduction elements $Q(x)$, the transverse shear force at position x, and $M(x)$, the bending moment at position x, can be derived starting from the knowledge of the resonance frequency and the associated mode shape $W(x)$. In case of a free-free beam with length L, the transverse shear force and the bending moment value are zero at the beam boundaries $x = 0$ and $x = L$. Physically this means that a beam element is considered with known boundary conditions W and M and that the value EI in the finite element is tuned such that the computed interior values of W match the measured values. The measurement techniques are discussed in the next paragraph.

4. EXPERIMENTAL MODAL ANALYSIS

A point to point measurement with a laser scanning vibrometer is used as a technique for the measurement of the modal amplitudes. The beam is excited acoustically at its first resonance with a small loudspeaker. An acoustical excitation is used in order to avoid physical contact of the excitation source with the test beam.

Figure 2 – The PSV (Polytec Scanning Vibrometer)

A Polytec Scanning Vibrometer (PSV) using a laser beam is used to measure the response of the beam to the excitation signal (Figure 2). The PSV is a full-field system for automated vibration measurement, mapping,

visualization and analysis. It measures the modal amplitudes point by point in a scanning mode. The laser beam is a non-contacting transducer and avoids the problem of mass loading of the test specimen with accelerometers. The Polytec Scanning Vibrometer software version 8.7.3.0 is used to analyse the signal. As laser scanning is a time-consuming test procedure, the department Mechanics of Materials and Constructions at VUB started looking for alternatives. The possibilities of shearography, mostly used as a qualitative measurement technique, for quantitative measurement purposes are now being explored. The technique using laser scanning vibrometer to measure modal amplitudes is used in the experiments discussed in the next paragraph.

5. EXPERIMENTS ON A COMPOSITE TEST BEAM

5.1. Description of the test specimen

An autoclaved epoxy prepreg material SE 84LV is used based upon a unidirectional High Elongation Carbon (HEC) with a modulus equal to 240 GPa±8GPa and a strength > 4.8 GPa (information from product catalog). The carbon weighs 0.3 kg/m². The fiber content of the composite specimen is approximately 60 %. Table 1 summarizes the measured dimensions and density of the test beams, labeled as CFRP-P3B08, CFRP-P3B09, CFRP-P3B11 and CFRP-P3B12. The first three specimens are used for the damage identification. Specimen CFRP-P3B12 is used for a tensile test. The cured layer thickness of the test beams is equal to 0.31 mm per layer. The test beam comprises 8 layer lamina $[(\pm45)_2]_S$. According to the processing notes provided by the manufacturer, cure can be achieved after 45 minutes at 120°. The curing cycle plot used in the autoclave for the test specimen is shown in Figure 3.

Table 1 – Dimensions and density of the composite test beams

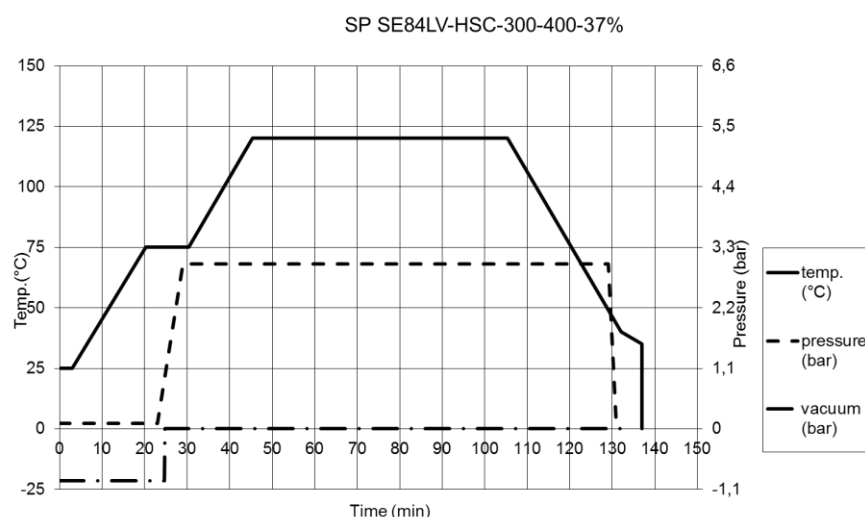| Beam	Length L [mm]	Width w [mm]	Mass m [g]	Density ρ [kg/m^3]
CFRP-P3B08	272.30	29.51	29.84	1493
CFRP-P3B09	272.21	29.51	30.08	1486
CFRP-P3B11	272.06	29.54	30.02	1490
CFRP-P3B12	271.95	29.54	29.73	1497

Figure 3 – Curing cycle plot

The first frequency of the undamaged beams is measured with the Resonalyser. A microphone is used instead of the piezo vibrometers because of the low weight of the beams. Table 2 summarizes the first frequency

determined from the Resonalyser test. Based upon the measured frequencies of the specimen, the Young's modulus E_{xx} in Table 2 can be calculated as:

$$E_{xx} = \frac{48\pi^2 L^3 m}{4.73^4 t^3 w} f^2 C \qquad (6)$$

where E_{xx} is the homogenized flexural modulus of elasticity, hereafter briefly named Young's modulus, m is the mass of the specimen, L is the length of the beam, t is the thickness of the beam, f is the resonance frequency of the beam and w is the width of the beam. The correction factor C depends on the ratio L/t and is equal to one since L/t is larger than 50 for these specimen.

Table 2 – Results of the Resonalyser test of the composite beam

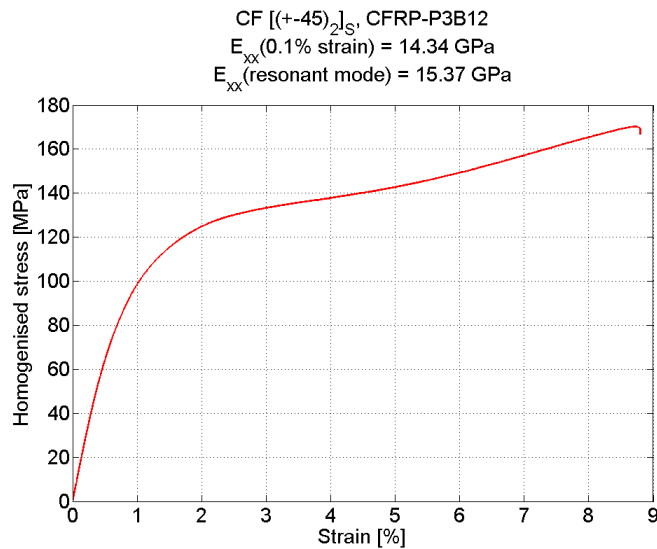| Beam	Frequency f [Hz]	Young's modulus E_{xx} [GPa]
CFRP-P3B08	108	14.7
CFRP-P3B09	109	14.5
CFRP-P3B11	109	14.6
CFRP-P3B12	110	15.4

Figure 4 – Stress-strain curve of the undamaged composite beam CFRP-P3B12

A tensile test is performed on the undamaged composite beam CFRP-P3B12. Figure 4 shows the stress-strain curve of the $[(\pm45)_2]_S$ laminate. A highly nonlinear behavior is observed. Tensile tests performed on unidirectional and $[(0/90)_2]_S$ lamina, using the same prepreg material SE 84LV, showed a linear behavior. The Young's modulus $E_{xx} = 15.4$ GPa determined from the Resonalyser test using the first frequency is similar to the result $E_{xx}(0.1\%) = 14.3$ GPa obtained from the experimental stress-strain curve. The homogenized stress at failure is equal to 169.4 MPa.

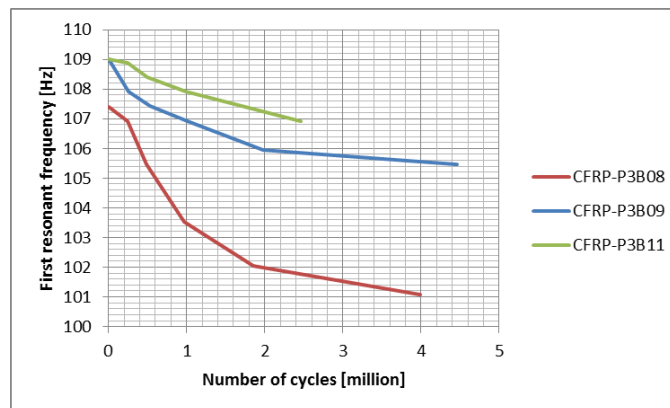## 5.2. Accelerated fatigue test

Figure 5 – Reduction in natural frequency in function of the number of loading cycles

Three specimens are fatigued on the shaker (see Figure 1) during several millions of loading cycles with an amplitude of 50 mm for specimen CFRP-P3B08 and 40 mm for specimens CFRP-P3B09 and CFRP-P3B11. Figure 5 shows the reduction of the resonance frequency of the beam during the shaker excitation due to the fatigue loading. A powerful fan was installed to cool the specimens, which lowered the temperature in the center of the beam to 35°C (ambient temperature was ~28°C during testing). The results of the monitoring of the temperature showed a constant temperature during the fatigue test. Figure 5 clearly shows a larger reduction of the natural frequency of specimen CFRP-P3B08 due to the higher stress level. Accelerated fatigue tests on the $[(0/90)_2]_S$ lamina and unidirectional lamina in the fiber direction did not show a property degradation after more than 25 million of cycles (more than 60 hours on the electro-magnetic shaker). Perpendicular to the fiber direction of the unidirectional lamina, brittle failure of the specimen occurred after 2 hours.

5.3. Experimental result on the damaged and the undamaged test beam

75 experimental points were used for the scanning. The measured first mode shape of the composite test beam was curve fitted with the 19th order Lagrange polynomial. A $M = 7$ point scanning element was used for the damage identification. The scan progressed from the left to the right with a step of 6 nodes; hence the sub domains had an overlap of 7-6 = 1 point. Figure 6 and Figure 7 show the stiffness distribution in the $[(\pm 45)_2]_S$ laminate. The results are shown in Figure 6 for specimen CFRP-P3B08 in the undamaged reference state D0 and after applying 4 million cycles with an amplitude of 50 mm (damage state D5) in Figure 7. The numbers of cycles applied for each damage state are summarized in Table 3. The identified stiffness pattern in the undamaged beam is obtained using the first bending mode shape in the inverse method. The order of magnitude of the amplitude of the mode shape should be high enough to obtain good results in the inverse method with respect to the signal to noise ratio. Tens of micrometers seems to be a good estimate for the amplitude but further research is needed. The solid line in Figure 6 and Figure 7 shows the homogenized beam stiffness values in bending computed with the resonance frequency of the first mode shape and is briefly called 'Analytical $E_{xx}I$'. The variation in the stiffness is due to the small changes in the thickness of the specimen over the length of the beam and in initial local material properties. The spots line is the identified local stiffness distribution. It can also be seen that the stiffness values identified in the zone of approximately 30% of the free ends of the beam are not useful. This is due to the lack of curvature (and hence information contents) of the observed mode shape in these zones. Figure 7 clearly shows a stiffness degradation after 18 hours or approximately 4 million of cycles. The effect is predominantly present at mid-span of the beam where the stress level is the highest during fatigue loading causing fatigue cracks.
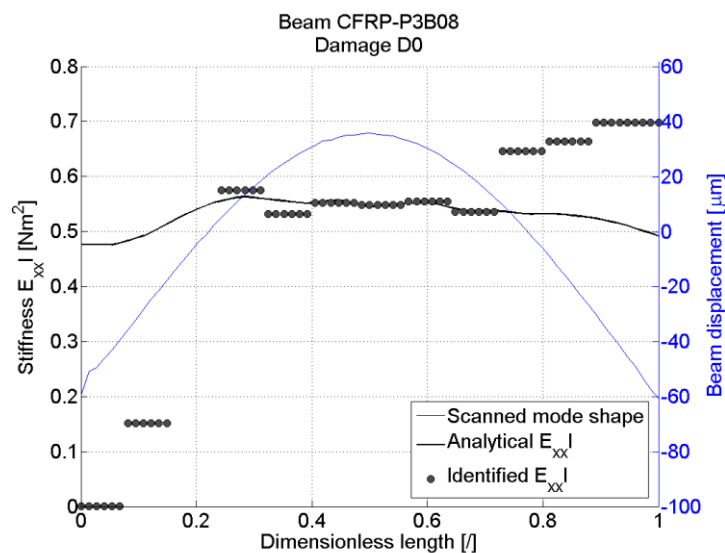
Figure 6 – Stiffness distribution in the undamaged composite beam CFRP-P3B08
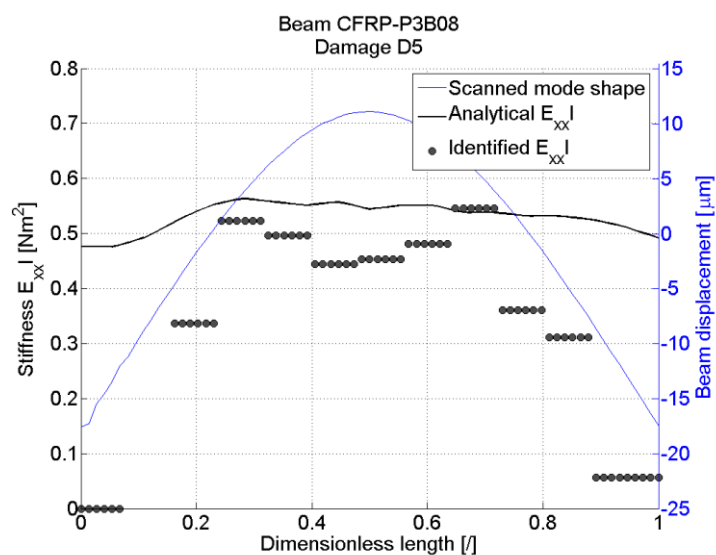

Figure 7 – Stiffness distribution in composite beam CFRP-P3B08 after 4 million of loading cycles with an amplitude of 50 mm

Table 3 – Number of cycles [million] and corresponding time [hour(s)] for each damage state

Damage state	Number of cycles [million]	Time [hour(s)]
D0 (undamaged)	0,00	0
D1	0,24	1
D2	0,48	2
D3	0,97	4
D4	1,85	8
D5	3,99	18

It can be seen in Figure 6 that the ('Analytical $E_{xx}I$' - calculated prior to scanning from the resonant frequency and the beam geometry) almost constant beam stiffness can be found back nearly correct using the scanning element technique. The stiffness in the beam intervals close to the free boundaries of the beam could not be identified because the mode shape does not have sufficient curvature at both extreme ends (and hence contains no information of the stiffness behavior). The results are not "perfect" because the displacement field obtained with the finite element method is piecewise linear varying and thus not continuous.
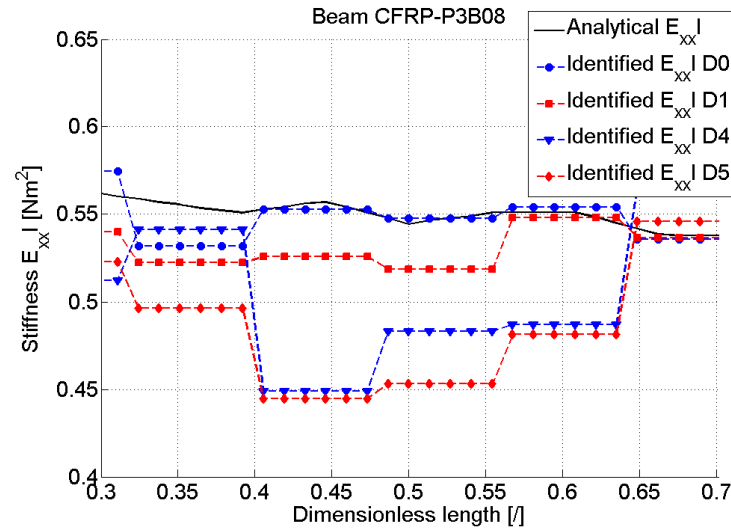

Figure 8 – Stiffness distribution in (a part of) the composite beam CFRP-P3B08 for the five damage states

Figure 8 shows the overall picture of the reduction of the beam stiffness values for different damage states in the fatigue assessment. Whereas Figure 6 and Figure 7 show the full length of the specimen (dimensionless length ranges from 0 to 1), Figure 8 only shows the part of the beam where sufficient curvature is present in the mode shape (dimensionless length ranges from 0.3 to 0.7). Only in this part of the beam the inverse method gives satisfactory results. The three damage states after 1 hour, 8 and 18 hours on the electro-magnetic shaker show a clear reduction in stiffness. The highest reduction value with an order of magnitude of 0.1 Nm^2 which corresponds to 20% reduction in $E_{xx}I$ is observed in the middle of the beam where the stress value is maximal.

6. FUTURE RESEARCH

To date, only carbon fiber reinforced polymers $[(\pm45)_2]_S$ laminates are extensively tested. Laminates with other directions and material composition will be prepared with a thorough inspection of the production according to the recommendations of the manufacturer (pressure, temperature, timing) and the damage identification results will be further validated and compared with data in literature. The sensitivity of local damage identification to the amplitude of the mode shape in the inverse method is further investigated. In a next phase, the fatigue damage assessment technique will be extended to plates.

7. CONCLUSIONS

A method is proposed to quantify the fatigue behavior of composite materials. Based on the frequencies of the undamaged beam, obtained from the Resonalyser test, and an analytical formula for the homogenized flexural modulus in bending, a stiffness distribution is obtained, taking into account the thickness variations of the specimen. Accelerated fatigue tests with an electro-magnetic shaker are performed on composite test beams with a layup $[(\pm45)_2]_S$. The reduction of stiffness in each local point of the test specimen is identified by scanning the amplitudes of the mode shapes with a laser vibrometer and applying an inverse identification algorithm. A clear reduction of the identified stiffness can be observed for the successive damage stages ranging up to 4 million

loading cycles. The faster and simpler fatigue tests in the proposed procedure to quantify local damage offer a cheaper alternative in fatigue assessment and local damage identification.

REFERENCES

[1]   W. H. M. van Dreumel, "Thermoplastic composites for aircraft applications. CORONET seminar - Design for Manufacturing of Thermoplastic Composites," Delft University of Technology, The Netherlands, Private Communication, 2004.

[2]   I. R. Farrow and J. B. Young, "Non-destructive test analysis and life and residual strength prediction of composite aircraft structures," *Composite Structures*, vol. 10, pp. 1-15, 1988.

[3]   P. McMullen, "Fibre/resin composites for aircraft primary structures: a short history, 1936-1984," *Composites*, vol. 15, no. 3, pp. 222-230, 1984.

[4]   E. Lamkanfi, W. Van Paepegem, J. Degrieck, C. Ramault, A. Makris, and D. Van Hemelrijck, "Strain distribution in cruciform specimens subjected to biaxial loading conditions. Part 1: Two-dimensional versus three-dimensional finite element model," *Polymer Testing*, vol. 29, no. 1, pp. 7-13, Feb. 2010.

[5]   E. Lamkanfi, W. Van Paepegem, J. Degrieck, C. Ramault, A. Makris, and D. Van Hemelrijck, "Strain distribution in cruciform specimens subjected to biaxial loading conditions. Part 2: Influence of geometrical discontinuities," *Polymer Testing*, vol. 29, no. 1, pp. 132-138, Feb. 2010.

[6]   K. L. Reifsnider, "The critical element model: A modeling philosophy," *Engineering Fracture Mechanics*, vol. 25, no. 5–6, pp. 739-749, 1986.

[7]   A. Smits, D. Van Hemelrijck, T. P. Philippidis, and A. Cardon, "Design of a cruciform specimen for biaxial testing of fibre reinforced composite laminates," *Composites Science and Technology*, vol. 66, no. 7–8, pp. 964-975, Jun. 2006.

[8]   F. Ellyin and M. Martens, "Biaxial fatigue behavior of a multidirectional filament-wound glass- fiber / epoxy pipe," *Composites Science and Technology*, vol. 61, 2001.

[9]   H. Sol and C. W. J. Oomens, "Material identification using mixed numerical experimental methods," in *Proc. of the Euromech colloquium, Kerkrade, The Netherlands*, 1997.

[10]   T. Lauwagie, H. Sol, G. Roebben, W. Heylen, and Y. Shi, "Validation of the Resonalyser method : an inverse method for material identification," in *Proceedings of ISMA2002*, 2002, pp. 687-694.

[11]   G. M. Seed, *Strength of materials*. Saxe Coburg Publications, 2000.

[12]   M. E. Friswell and J. E. Mottershead, *Finite element updating in structural dynamics*. Kluwers academic press, 1999.

[13]   W. Steinchen and L. Yang, *Digital shearography: theory and application of digital speckle pattern shearing interferometry*. SPIE Press, 2003, p. 310.

[14]   D. Francis, R. P. Tatam, and R. M. Groves, "Shearography technology and applications: a review," *Measurement Science and Technology*, vol. 21, no. 10, p. 102001, Oct. 2010.